XVII IAHR SYMPOSIUM
Beijing, China 1994

COMPARISON OF FLOW COMPUTATION RESULTS WITH EXPERIMENTAL FLOW SURVEYS IN A FRANCIS TURBINE

E. Parkinson, P. Dupont,
R. Hirschi, J. Huang, F. Avellan

IMHEF - EPF Lausanne
Switzerland

ABSTRACT

Three dimensional numerical tools are now commonly used in the design or analysis process of the internal flow of hydraulic machinery. As an illustration of the use of such tools to study the internal flow of a Francis turbine, the computational results obtained in all components of this turbine with an Euler equations solver and two Reynolds Averaged Navier Stokes equations solvers are discussed. The analysis process is illustrated and comparisons with experimental results obtained in the spiral casing and at the outlet of the guide vanes, runner and draft tube are presented.

RESUME

Les codes tridimensionnels font maintenant partie intégrante du processus de conception ou d'analyse de l'écoulement interne des turbomachines hydrauliques. L'utilisation de tels outils est illustrée sur le calcul de l'ensemble des composants hydrauliques d'une turbine Francis. Les résultats numériques obtenus avec un code de résolution des équations d'Euler et deux codes de résolution des équations de Navier Stokes sont comparés avec des mesures expérimentales effectuées dans la bache spirale, à la sortie des directrices, de la roue et du diffuseur.

A2

1. INTRODUCTION

Three dimensional numerical tools offer nowadays the opportunity to predict the behavior of hydraulic machines and are commonly used tools in the design process. The validation of such tools and the knowledge of their specific characteristics are therefore important. As an illustration of these remarks, a comparison between flow computation results and experimental data for a complete Francis turbine model is presented. The considered machine is a Francis turbine of specific speed v = 0.5. The corresponding hill charts and flow surveys were previously presented at the IARH Symposium in Belgrade [1]. Two types of three dimensional numerical codes are considered in this study. The EULER code of IMHEF [2] solves the Euler equations and the two codes FIDAP [3] of FDI and N3S [4] of EDF solve the Reynolds Averaged Navier Stokes equations (RANS).

This paper presents the comparison between the flow computation and the experimental data at nominal gate opening for various flow discharges. In a first part, all numerical and analysis tools are briefly presented. The main features of the turbine are then described before the presentation of the numerical computation results of each turbine component. An hydraulic analysis of these components is then proposed which leads to a global analysis of the turbine.

2. NUMERICAL ANALYSIS OF A TURBINE

2.1. Calculation process of a turbine component

The flow computation of any hydraulic component requires the definition of a computational domain where the internal flow of the component is calculated. For each component of the turbine, the velocity field is specified at the inlet plus specific code depending variables such as turbulence parameters. As a general rule, the inlet section is defined where velocity flow conditions are known and the outlet section as far as necessary from the real exit section of the considered element in order to minimize the effect of the downstream boundary conditions, as they are usually not exactly known. This is especially necessary when a constant pressure (Euler) or zero constraints (RANS) field is imposed in this section. The computational domain of each component is then discretised by defining the mesh. It is defined in a structured logical domain, except for the draft tube, with IMHEF meshing tools based on a 2D elliptic mesh generator [5] and conformal mappings. Specific tools are dedicated to spiral-casing geometries, with or without filets, distributors, runners and draft tubes. If RANS computations are required, filters are used to transform the EULER mesh into FIDAP or N3S meshes. Next, periodical and wall boundaries and steady or rotating parts are specified with the boundary conditions. The inlet and outlet initial conditions are then specified and the flow calculation is conducted until it is numerically converged. Its physical convergence is checked as described below.

2.2. Validation of a flow computation

The computation results are validated with an IMHEF hydraulic analysis package. As described in [6], the validation is performed by verifying the numerical and physical convergence of the calculation. The basic idea of this control is to survey, along any specific mesh line, the

A2

evolution of flow discharge, momentum for stationary parts, moment of momentum for rotating components and energy fluxes on mesh faces. For these momentum terms, the boundary of the computational domain is decomposed in two parts. First are considered the liquid faces, including inlet and outlet sections and secondly all solid boundaries. It is therefore possible to distinguish what is supplied to the system from what is transformed or restored by the system along the blades and walls, in terms of forces for stationary parts or torques for rotating components. For instance, in the case of a stationary component, the momentum equation is illustrated below:

$$\left[\int_A \vec{C}\,\vec{C}.\vec{n}\,dA + \int_{A_{i,e}} \left[\frac{p}{\rho} + \vec{g}.\vec{r}\right]\vec{n}\,dA\right] - \int_{A_w} \left[\frac{p}{\rho} + \vec{g}.\vec{r}\right]\vec{n}\,dA = \varepsilon + \int_A \frac{\bar{\bar{\tau}}}{\rho}.\vec{n}\,dA \qquad (1)$$

In the case of Euler equations, the Reynolds stress tensor, expressed in the right side of (1), is not introduced. The two left side terms of (1) are therefore equal, in the case of zero numerical losses, labeled ε in this equation. It is therefore possible to check the numerical validity of the computed pressure and velocity fields by verifying the zero value of ε. This equality is not anymore true with viscous equations where the Reynolds stress tensor is calculated.

2.3. Calculation process of the complete turbine flow

In order to complete the calculation of the turbine, as it is not yet possible to calculate all components all together, each part is calculated using an inlet velocity field predicted by the flow computation of the previous upstream component. For instance, the spiral casing flow calculation predicts an average absolute flow angle profile upstream of the stay vanes. Using this profile as an inlet velocity field, a single blade to blade channel of the distributor is calculated at a given gate opening, because of periodicity. The process is repeated to calculate the runner and draft tube internal flows. As an overlap exists between the computation domain of two consecutive elements, the coupling is controled by comparing numerical flow surveys at the same location with both numerical solutions.

3. FRANCIS TURBINE MODEL

3.1. Geometrical features

The model corresponds to a Francis turbine of medium specific speed, $\nu = 0.5$. This model has been extensively studied at IMHEF for research purposes. The spiral casing, presented at Figure 1, is of the Piguet type. The stay ring, illustrated in Figure 1, is made of 24 stay vanes and the distributor, also presented in Figure 2, of 24 guide vanes. The hydraulic profile of the guide vanes is symmetric. The relative guide vane opening α is defined with reference to the closed position of the guide ring. The absolute guide vane opening, at closed position, is $\gamma_{oc} = 5.39°$. The runner, designed and built at IMHEF, has 13 blades. The runner outlet external diameter is 0.4 m. The draft tube has an internal pillar at its non symmetrical outlet section.

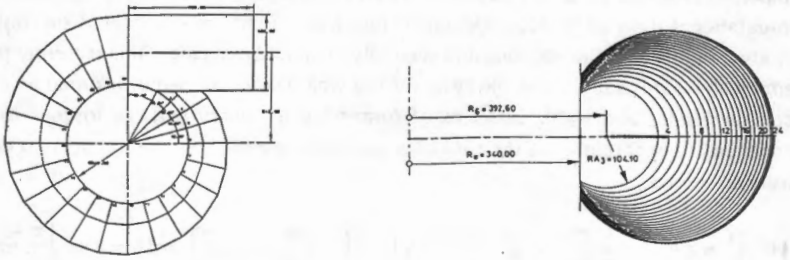

Figure 1 : Geometry of the 0.500 Francis turbine

3.2. Hydraulic features

The characteristics and the efficiency hill chart are presented in Figure 2. A maximum efficiency η of 0.93 is measured at $\alpha = 25°$. The reference section for head measurements is at the outlet of the draft-tube. The operating conditions are referenced with non dimensional coefficients φ and ψ defined as $\varphi = \frac{Q}{\pi\ \omega\ R^3}$ and $\psi = \frac{2\ E}{\omega^2\ R^2}$ where R is the external outlet radius of the runner.

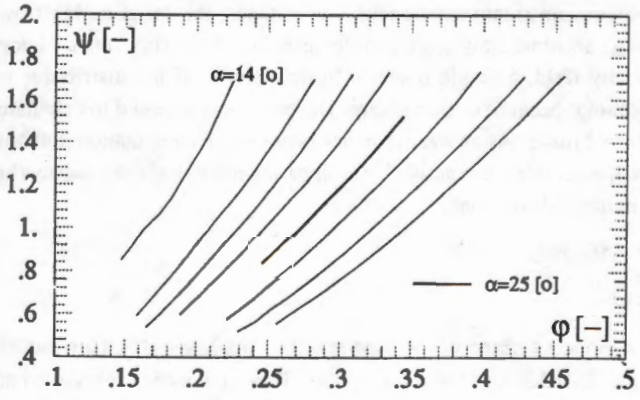

Figure 2 : Hill chart

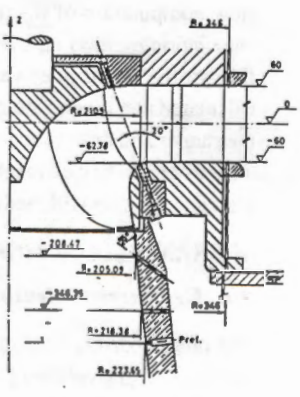

Figure 3 : Flow surveys sections

3.3. Experimental data

The flow surveys, conducted with five hole probes, [2] presented in this paper were measured at the inlet of the stay vanes (8 sections, Figure 1), at the outlets of the guide vanes, runner and draft tube (4 sections). These sections are described in Figure 3. Five operating conditions,

labeled A to E in the following text are studied (φ = 0.213, 0.244, 0.278, 0.299 and 0.320) at nominal gate opening, $\alpha = 25°$.

4. FLOW COMPUTATIONS

4.1. Codes used

Three codes were used for this study. The EULER code [1], [7], developed at IMHEF, allows the computing of incompressible, inviscid and steady state flows in a stationary or rotating frame of reference. The meshes are structured. It uses a finite volume discretization scheme. The FIDAP fluid dynamics analysis package is a general purpose finite element code to simulate three dimensional transient or steady, compressible or incompressible, laminar or turbulent flows. N3S of EDF-Simulog is also a general purpose finite element code with specifications similar to FIDAP. A specific turbomachinery version of N3S is designed to treat rotating components. Both RANS codes use k-ε turbulence models.

4.2. Description of flow computations

In order to calculate the complete turbine, all converging components, thus including the spiral casing, the distributor and the runner, are calculated with the EULER code. As no viscous effects are taken into account, the computed flow is independent of the operating conditions for all stationary parts. A single calculation is therefore sufficient for the spiral casing and the distributor, considering a single gate opening. On the opposite, each considered operating condition asks for a specific RANS computation in all components in order to estimate the losses related to Reynolds effects.

4.3. Mesh and computing specifications

As detailed earlier, all meshes are structured, except for the draft tube. Two transversal sections of the mesh of the spiral casing are presented in Figure 4. The real geometry of the filets is used. A top view of the distributor mesh is also presented. Periodicity is applied to the computing domain to ease the understanding of the geometry.

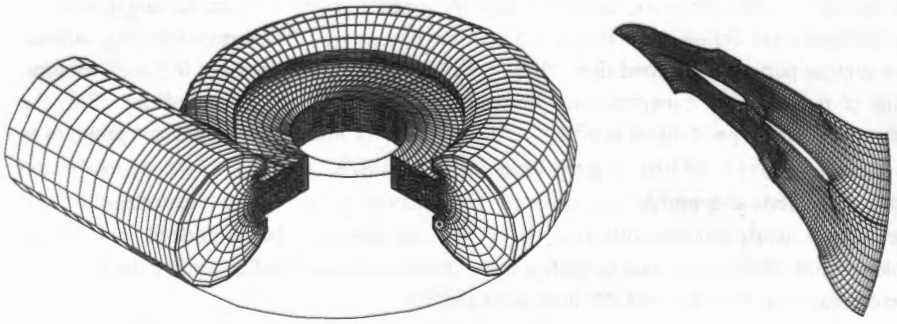

Figure 4 : Meshes of the turbine components

The specifications of these meshes are detailed in the following table.

	Euler	FIDAP	N3S
Mesh Elements	8 node bricks	8 node bricks	10 nodes tetraedra
Spiral Casing	67'500 nodes	67'500 nodes	- - -
Distributor	22'500 nodes	22'500 nodes	32'105 nodes
Runner	35'530 nodes	27'000 nodes	- - -
Draft tube	- - -	20'000 nodes	- - -

Figure 5 : Numerical and mesh specifications

These meshes are not necessarily optimized for the considered calculations. The important point is to be able to qualify the results obtained with a defined margin of error for a given mesh without spending too much time in designing an ultimate optimized mesh. This is made possible with the control process described earlier.

5. RESULTS AND ANALYSIS

5.1. Spiral casing

A quality factor of the spiral casing is determined by the uniformity of both discharge and absolute flow angle distributions along the peripheral angular position at the leading edge of the stay vanes. These two criteria are used to characterize the flow computations. In Figure 6, the vertical absolute flow distribution computed with EULER and FIDAP are compared to experimental measurements. The corresponding discharge and average flow angle distributions along θ are presented in Figure 7. The discharge is overestimated by both computations at the inlet of the spiral casing near the tongue which is modelized by a solid wall condition followed by connected cells. This overestimation is related to the absence of stay vanes, which are not taken into account in the constant pressure outlet condition. Of course, a solution is to include the stay vanes in the computing domain. It appears however as very time consuming in terms of unstructured mesh definitions and required numbers of nodes [5]. The most interesting solution is to impose permeability conditions at the outlet related to loss behaviors in the distributor, either computed [6] or experimentally determined. The Euler flow is over influenced by the filets, generating a parabolic α profile. The Navier Stokes computations avoid this problem as the boundary layer is treated. A good behavior of the FIDAP results is observed as the non symmetrical vertical α profile is reproduced. The behavior of the average $\bar{\alpha}$ Euler results is of interest as a nearly constant difference of 5° with experimental data is noticed. The Navier Stokes results are more difficult to qualify as the profile is too much influenced by the discharge overestimation at the inlet (θ=355°) as observed in Figure 7.

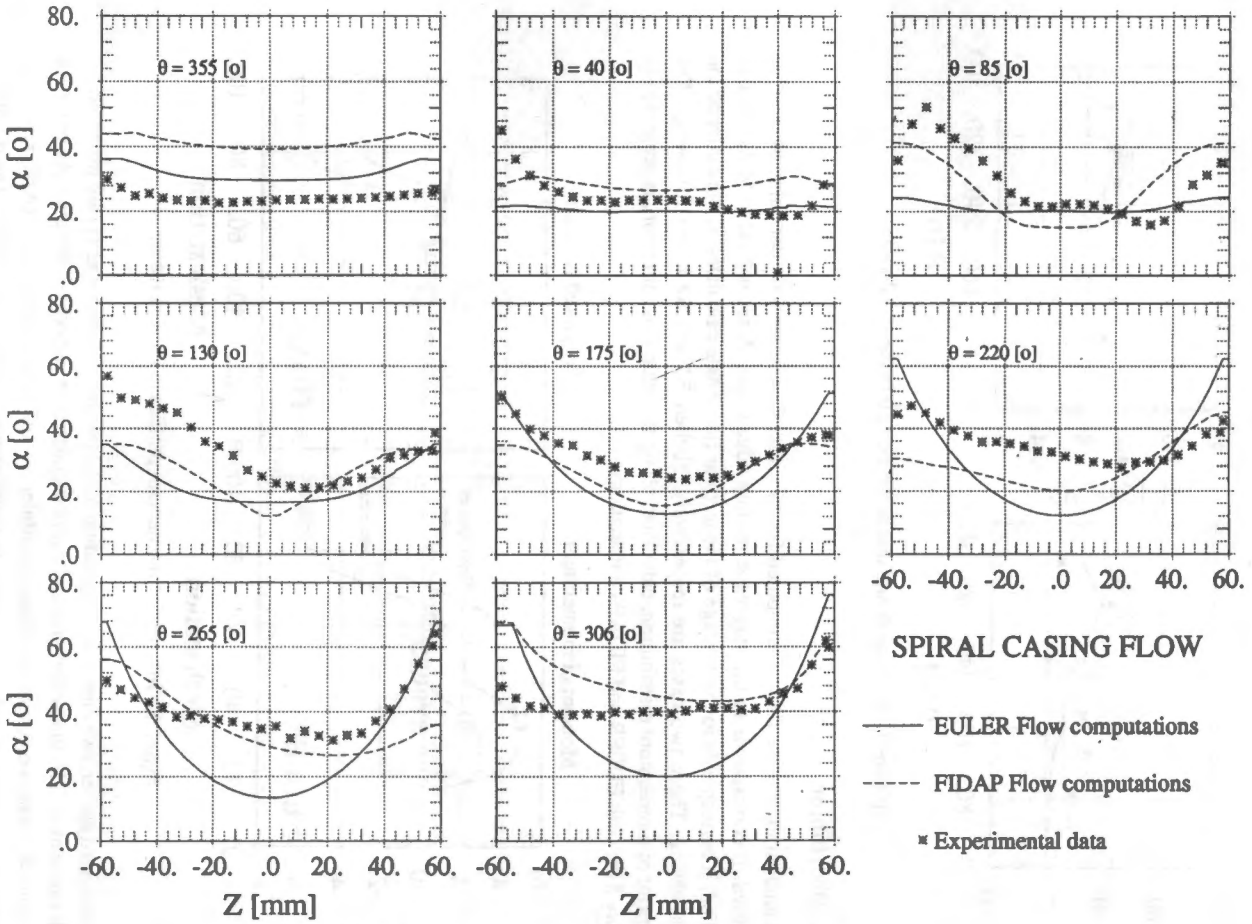

Figure 6 : Comparison of numerical and experimental flow surveys in the spiral casing

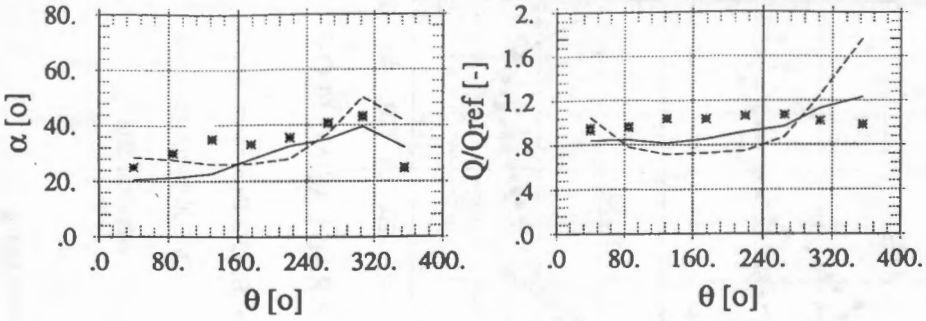

Figure 7 : Average α and discharge along θ in the spiral casing

5.2. Distributor

The internal distributor flow is computed for two inlet flow angles. A first value of 36.8° is imposed. It corresponds to the stay vane leading edge angle. A second value of 29° is also applied. It corresponds to the average of the angular flow angle calculated at the outlet of the spiral casing. These two cases are respectively labelled B1 and B2 in the following. The momemt of momemtum distribution, calculated along the main flow direction, is presented in Figure 8 for both EULER and FIDAP computations.

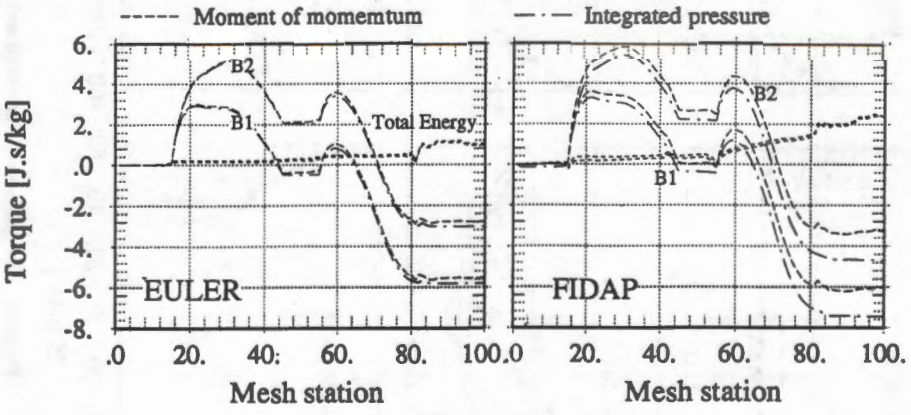

Figure 8 : Moment of momentum profiles in the distributor

As explained earlier, two curves corresponding to the two left side terms of (1) are observed for each calculation. The integrated pressure curve is constant in periodical domains. As observed in Figure 8, these two curves are identic for Euler calculations as opposed to RANS results, as the Reynolds stress tensor is not included in the momemt of momemtum curve. The difference between the two curves is therefore an indicator of the Reynolds stress tensor contribution plus numerical losses in this element. It explains the identical outlet level of the moment of

momemtum term in both EULER and FIDAP calculations at station 100. Considering the shape of the curves between stations 15 and 45, which correspond to the stay vanes duct, their loading is higher for the non zero incidence (case B2). The loading profile of the guide vane, from stations 55 to 85, is identical in both cases as the flow at the outlet of the stay vanes is independant from the inlet flow angle. The latter point is confirmed in Figure 9 where the numerical results of both cases B1 and B2 are compared to experimental data at the outlet of the guide vanes.

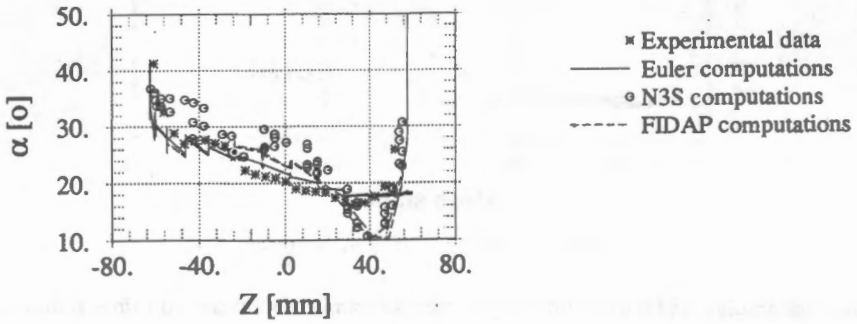

Figure 9 : Flow surveys at the outlet of the guide vanes

The continuous curves, representing the Euler computations, are similar in both cases. Euler computations predict correctly the experimental results except in the vicinity of the walls as no boundary layer is taken into account in the calculation. The results of FIDAP tend to overpredict α nearby the top wall. This is related to the size of the mesh cells in this region which are not optimized for a Navier Stokes calculation. A similar behavior is followed by the N3S results. Mesh refinements are needed at the outlet of the distributor duct because of its strong curvature. The distributor flow computation enables the defining of the inlet velocity flow field for the runner calculation. It is calculated from velocity profiles obtained at the outlet of the guide vane.

5.3. Runner

The runner internal flow is calculated for all five operating conditions with the EULER code and at best operating conditions C with FIDAP. The torques obtained by integrating the pressure on the blades and by integrating the moment of momentum along the mesh stations are presented in Figure 10. Different meshes are used for EULER and FIDAP computations. For the EULER mesh, the leading edge of the runner starts at station 21 and the trailing edge is at station 56. These curves illustrate the energy transfer between the flow and the blades. An incidence default is observed for operating conditions A and B near the leading edge where a negative transfer occurs. Oscillations are observed at the trailing edge, due to unsatisfactory mesh definition. The calculated values are presented in Figure 11 where the characteristics $\psi.\eta$ of the sole runner are presented. The measured characteristics are in between the two pressure and momentum values of torque calculated with the Euler results. The difference between the two computed values is a quality indicator of the calculations. A perfect result would be a zero difference. In our case, it would thus be necessary to refine the mesh at the trailing edge.

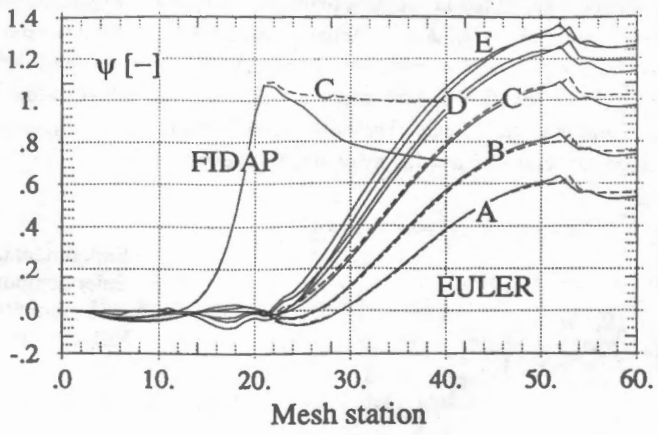

Figure 10: Energy transfer in the runner

Calculated absolute and relative flow angles are also compared to measured values at the outlet of the runner in the downstream cone in Figure 11. The cone represents a difficulty for the computation as it is a diverging element and a pressure condition is imposed at the outlet section. Of course, the Euler calculation is not able to predict the behavior of the flow in the vicinity of the rotating axis. However, a good agreement of β values is observed. Absolute flow angles α are systematically 10° underestimated.

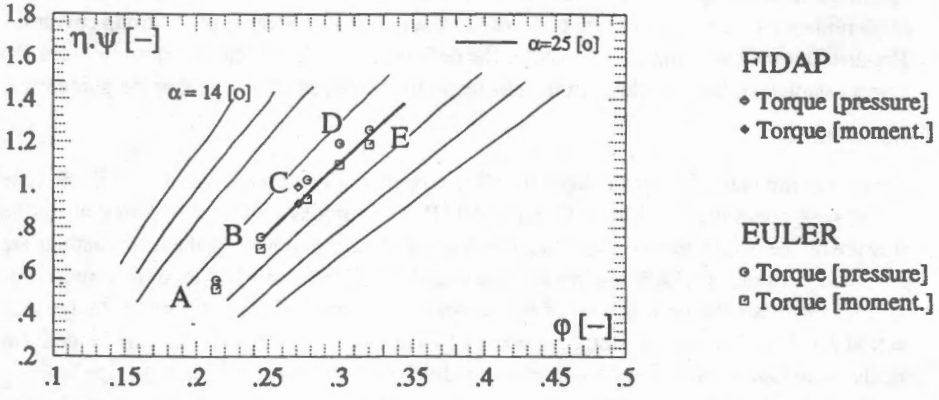

Figure 11: Runner characteristics

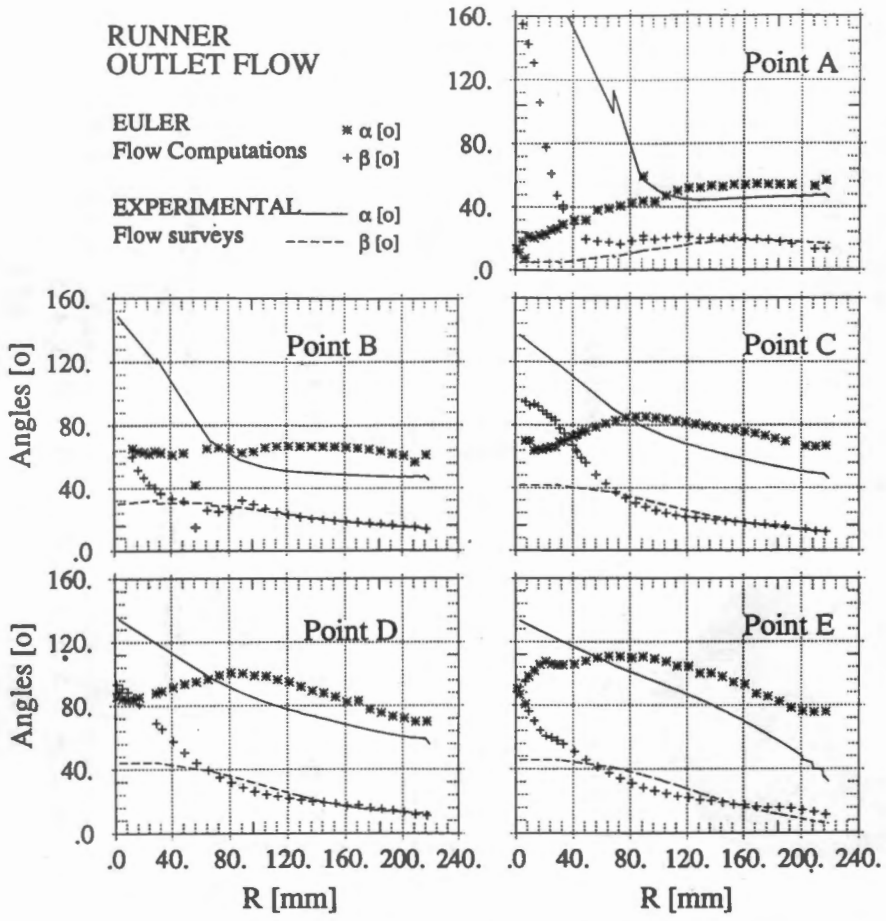

Figure 12: Absolute and relative flow angles at the outlet of the runner

5.4. Draft tube

As Euler or FIDAP flow surveys are not fully satisfactory at the runner outlet, an experimental flow survey is used as an inlet velocity condition for the computation with FIDAP of the draft tube. The results presented correspond to the best operating conditions of the turbine. A specific unstructured mesh is defined. Normalised experimental velocity profiles at the outlet of the draft tube are compared to computational results in Figure 13 at three vertical stations labelled DT1, DT2 and DT3. The Navier Stokes results predict correctly the behavior of the flow, in regards of the measurement discrepancy.

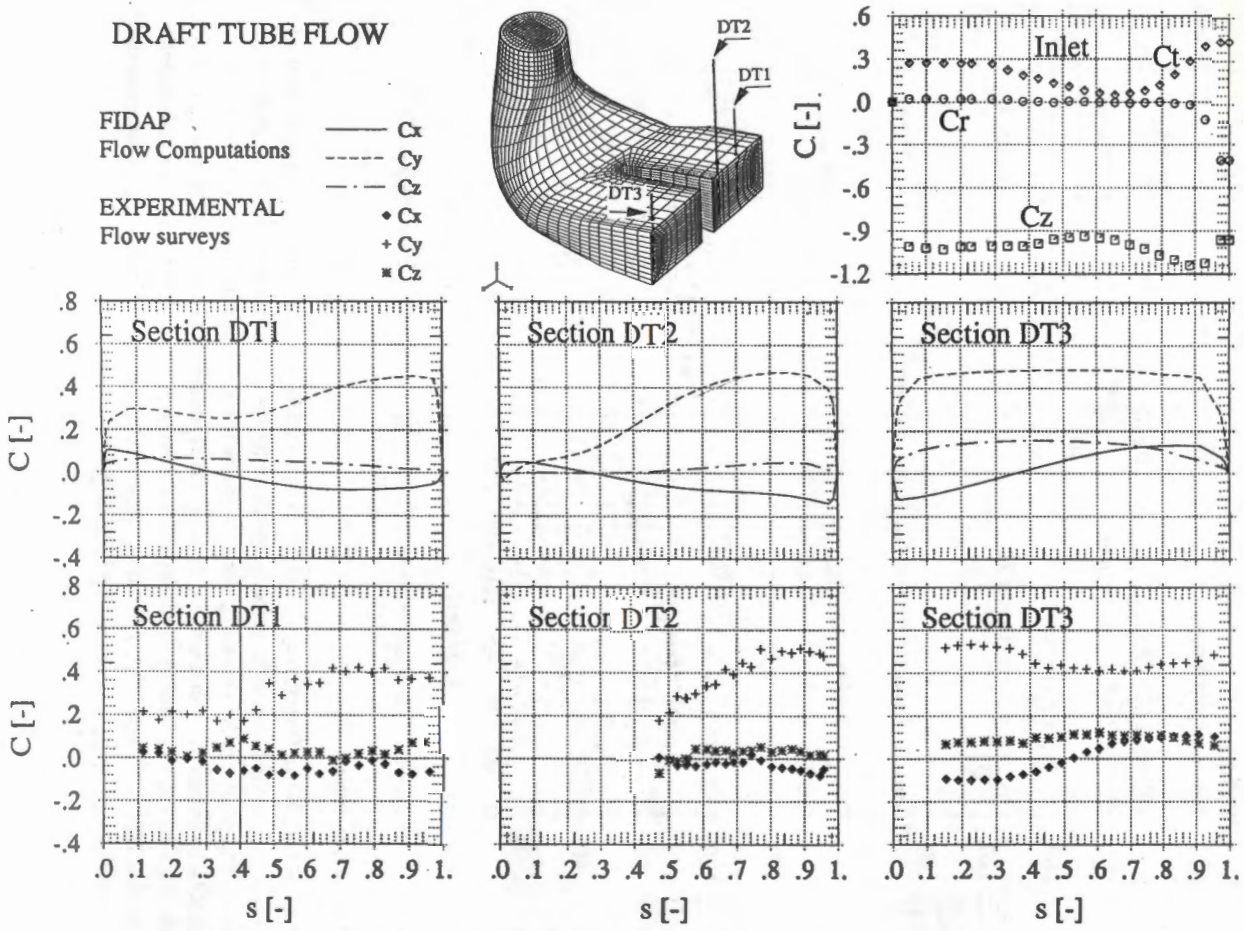

Figure 13 : Comparison of numerical and experimental flow surveys in the draft tube

6. CONCLUSION

The use of three dimensional codes to predict the internal flow of turbine components is highly dependent of analysis tools. Physical convergence of a flow computation is not necessarily checked eventhough numerically converged, as illustrated on the distributor and runner geometries. A global analysis of the behavior of the calculated component is also of interest before studying more deeply local values of velocity or pressure. The good results obtained with the EULER code are emphazised, compared to the cost of Navier Stokes computations and their sensivity to mesh definition.

ACKNOWLEDGMENTS

The authors wish to thank for its support the CERS funds. This work is supported fiancially by the Sulzer Escher Wyss and Hydro Vevey S.A. The work of all colleagues of the technical staff of IMHEF Test Rigs is also acknowledged. The authors wish to thank Jean François Combes of EDF for his help in achieving the N3S computations.

REFERENCES

[1] Eriksson L.E., Rizzi A., Therre J.P. - *Numerical solution of unsteady incompressible Euler equations applied to water turbines.* - AIAA-84-2145

[2] Haroutunian V., Engelman M.S. - *Two-equation simulations of turbulent flows : a commentary on physical and numerical aspects* - ASME Winter Annual Meeting, FED-Vol.171, Advances in Finite Element Analysis in Fluid Dynamics, pp.95-105, Nov.28-Dec.3, 1993, New Orleans, USA

[3] Chabard J.P., Pot G., Martin A. - *Industrial application of N3S finite element code* - ASME Winter Annual Meeting, FED-Vol.171, Advances in Finite Element Analysis in Fluid Dynamics, pp.1-9, Nov.28-Dec.3, 1993, New Orleans, USA

[4] Santal O., Avellan F. - *Hydraulic analysis of flow computation results* - IAHR International Symposium, Sao Paulo, Brazil, 1992.

[5] Avellan F., Dupont Ph., Fahrat M., Gindroz B., Henry P., Hussain M., Parkinson E., Santal O. - *Flow survey and blade pressure measurements in a Francis turbine model* - IAHR International Symposium, Belgrade, 1990.

[6] Dupont Ph., Parkinson E. - *Cavitation development in a centrifugal pump : Numerical and model test predictions* - ASME Winter Annual Meeting, FED-Vol.177, Cavitation Inception, pp.63-72, Nov.28-Dec.3, 1993, New Orleans, USA

[7] Soares Gomes F.J. - *Modélisation tridimensionnelle des écoulements dans les bâches et volutes* - Thèse de doctorat INPG - Oct.1993

[8] Vu T.C., Shyy W. - *Performance prediction by viscous flow for Francis turbine runner* - IAHR International Symposium, Sao Paulo, Brazil, 1992.